Geomorphology 185 (2013) 96–109

Contents lists available at SciVerse ScienceDirect

Geomorphology

journal homepage: www.elsevier.com/locate/geomorph

Impact of atmospheric circulation patterns on coastal dune dynamics, NW Spain

R. González-Villanueva [a,*], S. Costas [a], M. Pérez-Arlucea [b], S. Jerez [c], R.M. Trigo [c,d]

[a] Unidade de Geologia Marinha (UGM), LNEG, 7586, Lisbon, Portugal
[b] Dpto. Xeociencias Mariñas e O.T. (XM1), 36310, Universidade de Vigo, Spain
[c] Instituto Dom Luiz, Universidade de Lisboa, 1749-016 Lisboa, Portugal
[d] Departamento de Engenharias, Universidade Lusófona, 1749-024 Lisboa, Portugal

ARTICLE INFO

Article history:
Received 3 August 2012
Received in revised form 13 December 2012
Accepted 16 December 2012
Available online 24 December 2012

Keywords:
Aeolian activity
Blowout
Climate variability
Dune stabilization
SW Europe

ABSTRACT

Dunes in temperate latitudes have experienced a significant stabilization in recent times, essentially as a consequence of the expansion of dense vegetation cover. Yet, the causes for this gradual stabilization as well as the causes promoting antecedent aeolian mobilization remain poorly understood. The Traba coastal dune field, located in NW Spain, was examined to explore the causes inducing aeolian activity and subsequent stabilization since 1940. Morphological changes were identified through the combination of aerial photographs and geophysical techniques. Local wind field regimes were simulated using a regional climate model to obtain the variability of the most relevant modes of atmospheric circulation in the North Atlantic and European regions; North Atlantic Oscillation (NAO), Eastern Atlantic (EA) and Scandinavian (SCAND). This allows us to identify the impact of these circulation modes over dune dynamics. Results document an episode of aeolian activity during the 1950s followed by a gradual stabilization and fixation of the dune coincident with a decrease on storm and wind intensity. Yet, aeolian sand movement remained active in small areas (blowouts), occurring mainly during the summer. NE winds associated with a negative phase of the EA explain the movement of sand within the dune field under favorable conditions of sand supply. On the other hand, sand supply to the dune field from the beach was promoted by NW winds coincident with the summer negative phase of NAO. During winter, the negative NAO favored frequent SW winds associated with the passage of intense storms, which in turn explain sand remobilization from the beach making sediment available for the NW winds to blow inland. With this work, it is proven that to understand past and future aeolian activity requires critical consideration of the variability and impact of the two principal modes of atmospheric circulation in the North Atlantic (NAO and EA). The SCAND mode explaining a lower percentage of the local wind field variability was also included to achieve higher significance levels of explained variance.

1. Introduction

Aeolian dunes are the result of complex histories of alternating events of sand drift and dune stabilization. Natural dune stability and mobility are influenced by three major factors: climatic variables (i.e. wind, precipitation, moisture), sediment characteristics (i.e. availability, grain size) and vegetation cover (Klijn, 1990; Pye, 1993). Episodes of aeolian activity have been linked repeatedly to an increase of sediment supply (Davidson-Arnott and Law, 1996; Aagaard et al., 2004) and changes in climate conditions (Gaylord and Stetler, 1994; Tsoar et al., 2009). On the European coasts, enhanced storminess has often been invoked as a major causal factor for the initiation of dune activity (Clemmensen et al., 1996; Wilson and Braley, 1997; Wilson et al., 2001; Clarke et al., 2002; Clarke and Rendell, 2009; Costas et al., 2012). However, the actual mechanism responsible for the reactivation of aeolian activity in coastal systems remains poorly understood (Bailey and Bristow, 2004; Buynevich et al., 2007; Girardi and Davis, 2010). Currently, most European coastal dunes have undergone a progressive stabilization as vegetation cover expanded, but the causes behind such a landscape shift remain under debate (Bailey and Bristow, 2004; Costas and Alejo, 2007; Arens et al., 2008; Jackson and Cooper, 2011). Several factors have frequently been inferred as possible causes for the growth of vegetation in coastal dunes, including anthropogenic pressure (i.e. changes in land use, landscape fixation, introduction of non-native species); semi-natural factors (i.e. crashing rabbit populations, eutrophication) or climatic-derived changes (i.e. enhanced CO_2 concentration and temperature, diminished wind and storminess); see Provoost et al. (2011) for a review.

From a climate variability perspective, increased emphasis has been put on the role played by the most important large-scale mode of atmospheric circulation in the North Atlantic. The climate of Galicia, located in the northwestern corner of the Iberian Peninsula has been reviewed in detail in a recent special issue (Gimeno et al., 2011). It has been noticed that a relatively small number of these modes are responsible for a large fraction of the wind and precipitation

* Corresponding author.
E-mail address: rita.gonzalez@lneg.pt (R. González-Villanueva).

0169-555X/$ – see front matter © 2012 Elsevier B.V. All rights reserved.
http://dx.doi.org/10.1016/j.geomorph.2012.12.019

fields (Gómez-Gesteira et al., 2011). Among these large-scale patterns of atmospheric circulation defined for the Northern Hemisphere, the role played by the three most important modes over the North Atlantic and European sectors must be emphasized; namely, the North Atlantic Oscillation (NAO), the Scandinavian (SCAND) pattern and the Eastern Atlantic (EA) pattern. Considering the impact that the NAO has on the position of the zonal storm track within the North Atlantic region (Osborn et al., 1999; Goodess and Jones, 2002), some works have explored the relation between the variability of the NAO and the changes in coastal systems (Lebreiro et al., 2006; Costas and Alejo, 2007; Chaverot et al., 2008; Pye and Blott, 2008). However, these works obtained relatively modest levels of correlation with the NAO index and have never considered the impact of other modes of circulation that, as for the case of the EA pattern, may represent a significant contribution for the precipitation over northern Iberia (Sáenz et al., 2001; Trigo et al., 2008). In addition, the SCAND pattern is associated with a strong positive pressure anomaly centered over Scandinavia and western Russia and negative anomalies over the Iberian Peninsula, inducing important precipitation anomalies in both western and eastern Mediterranean regions (Quadrelli et al., 2001; Trigo et al., 2008).

In order to further explore the impact that the patterns of climate variability may have on coastal systems in the SW of Europe we investigate the history of aeolian activity in the Traba dune field (NW Spain) during the last 70 years in relation to the local wind field. With the aim of obtaining a better correlation between the coastal evolution and the modes of atmospheric circulation, the NAO, the SCAND and EA are included in the analysis of wind field patterns. The study area has recently experienced a gradual stabilization of the dune field following a period of intense mobilization. Due to its recent evolution, Traba represents a suitable example to illustrate the factors triggering the alternation of erosion/stabilization pulses within the aeolian dunes. Therefore, the main objectives of this work are twofold:

1) To examine the evolution of the dune system landscape at a decadal timescale since the 1940s using aerial photography and climatic data, particularly wind power. The same methodology was used to study recent aeolian activity with the implementation of a Ground Penetrating Radar (GPR).
2) To assess the role played by the most important modes of large-scale atmospheric circulation (NAO, EA and SCAND) using the longest high-resolution (10 km) dataset available. This will be done at the individual pattern level but also simultaneously, with appropriate regression models that consider the contribution of all 3 modes, distinguishing their respective and interrelated determinant influences on the wind field with the observed evolution of the coastal system.

2. Regional settings

Traba is a coastal system located in the northwest of the Iberian Peninsula (Fig. 1). The system is formed by a 2.5 km-long and 400 m-wide sand barrier, with a NE–SW orientation. The seaward region of the barrier comprises a wide beach, with well-developed beach cusps, capped by a low dune interrupted by overwash channels (Devoy et al., 1996). To the south, the sand barrier is backed by a freshwater shallow coastal lagoon with a 2 m maximum water depth. Two small fluvial streams flow into the lagoon (Bao et al., 2007), which is also connected to the open ocean through an intermittent inlet during storm events (Vilas and Rolán, 1985). Bao et al. (2007) dated the onset of the sand barrier in Traba at around 4920 ± 50 ^{14}C years BP, and Devoy et al. (1996) suggested the landward migration of the barrier from 1520 ± 70 ^{14}C years BP to the present with small phases of sand stability and instability. The authors suggest alternating periods of vegetation growth and relative environmental stability with pulses of sand drift. Yet, the actual driving mechanisms and the ages of these pulses remain unclear.

The coastal dune consists of a sparsely vegetated foredune ridge reaching elevations higher than 14 m above ADS (Alicante Datum of Spain, a datum based in mean sea level at Alicante). The foredune ridge is cut by several blowouts (Fig. 1). Inland of the foredune crest, large vegetated depressions located around 3 m above ADS separate the lagoon from the present coastline. Isolated active

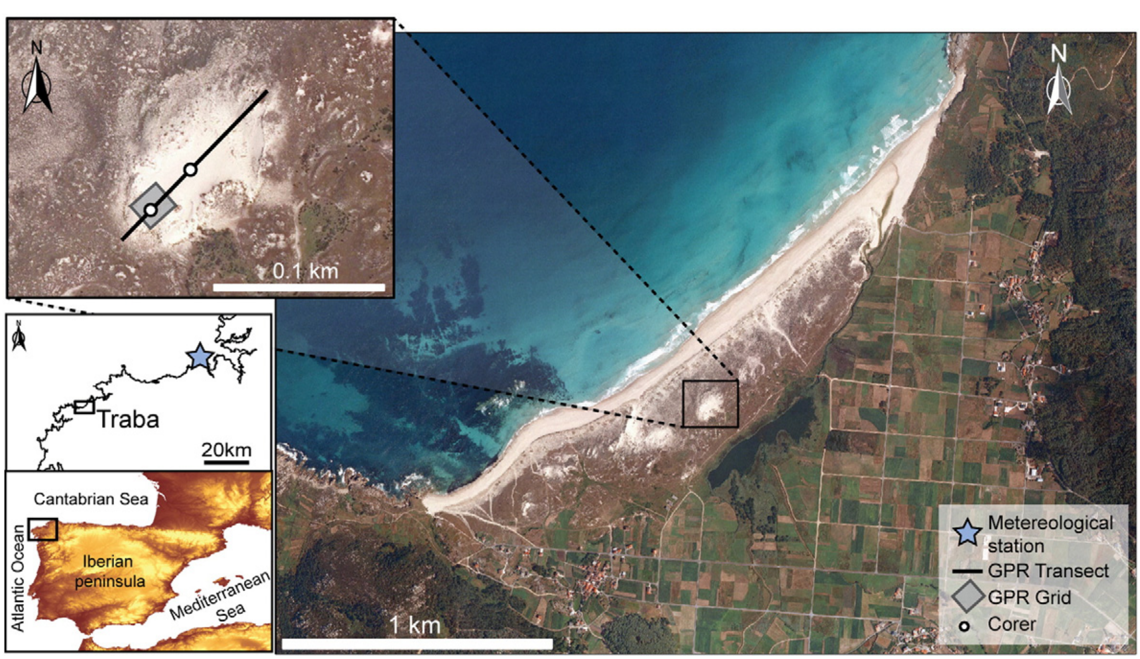

Fig. 1. Location of Traba sedimentary complex in NW Spain showing the location of the 2D transect, 3D grid survey and collected sediment corers. The star represents the location of A Coruña meteorological station.

aeolian features located about 10 m above ADS cross these depressions heading south (Fig. 1). Present vegetation cover in the foredune and mobile dunes is dominated by *Elytrigia juncea*, *Ammophila arenaria*, *Cakile maritima*, *Calystegia soldanella*, *Linaria polygalifolia* and *Eryngium maritimum*, while *Euphorbia portlandica*, *Pancratium maritimum*, *Calystegia soldanella*, *Malcomia littorea* and *Romulea clusiana* dominate the vegetation cover on fixed dunes and *Juncus maritimus*, *Frankenia laevis*, *Sedum album* and *Ornithogalum broteroi* in low lying areas.

The coast is within the mesotidal regime with a mean spring tidal range of 4 m. The highest astronomical tide (HAT) is around 2 m above ADS. However, according to the data collected by our team in recent years in the study area, water levels may reach 3 m above ADS during storm surges. The water level in the lagoon is around 2 m above ADS, but it can reach values of 3.2 m during rainfall periods, leading to the flooding of dune field depressions. The average temperature in the area ranges from 10–12 °C in winter and to 20 °C in summer, and the average rainfall is around 1300 mm/yr (Martínez Cortizas and Pérez Alberti, 1999). Prevailing winds in the area are from the NE and ENE, while the strongest winds blow from SW and SSW without a direct impact in the study area due to the shelter by orographic highs. Being located at the southern limit of the North Atlantic (NA) storm track, the region is particularly sensitive to interannual shifts in the trajectories of the mid-latitude cyclones, which are in turn controlled, to a large extent, by the NAO. The NAO is associated with the strength of the meridional pressure gradient along the NA. Most works for Iberia or the Mediterranean region have focused on the impact of the NAO during the winter season when its impact is greatest in precipitation (Rodriguez-Fonseca and de Castro, 2002; Trigo et al., 2004). However, as explained above, other major modes of atmospheric variability, namely the EA and the SCAND patterns, must be included on any analysis of climate variability in the NA to understand the complete picture (Trigo et al., 2008).

3. Methodology

Aerial imagery, flooding simulations and GPR surveys were conducted in Traba to explore the recent changes in this coastal system. Conciliating these results with observed and simulated wind data which are related to the NAO, EA and SCAND teleconnection modes, was considered, to delineate and understand the causes of the favorable wind regimes during different episodes of mobility or stabilization of the dune.

The temporal range of aerial imagery and that of observed and simulated wind data are not exactly coincident due to limitations in data availability. The first aerial photography was taken in 1945, thus this date imposes the lower limit of the temporal scale in this study. To establish a relation between the morphological changes and the wind regime we used the observed data of the A Coruña meteorological station since 1940. In addition, we have explored the effect of the atmospheric circulation modes over the wind field in the study area using a high resolution simulation (10 km) from 1959 to 2007, including surface winds. In this case, the temporal range is limited to the availability of the temporal data in the ERA-40 re-analysis dataset used in the simulation. Nevertheless, the obtained results allow the understanding of the morphological changes in the periods without simulated data.

3.1. Aerial imagery and flooding simulations

Nine vertical aerial photographs obtained between 1945 and 2008 (1945, 1957, 1971, 1978, 1985, 1989, 2002, 2003, and 2008), with spatial scales ranging from 1:20,000 to 1:5000, have been used to acquire information on dune growth, reactivation and stabilization. The photographs were digitized and processed using ArcGIS to produce georeferenced images. At least 20 landmarks were identified on each photograph, and root mean square errors of <2 m were considered acceptable. The reference system used was ED50, UTM zone 29N. The comparison and superimposition of successive corrected images combined with GPR allowed a dynamic visualization of dune development and evolution through time (Bailey and Bristow, 2004; Costas et al., 2006; Hugenholtz et al., 2008; Buynevich et al., 2010). For that, the entire system was divided into five surficial units: beach, active dune, vegetated dune, flooded areas and marsh. The units were identified and mapped in all aerial photographs to analyze the temporal changes in the surface of every unit. Temporal changes in the percentage of the vegetated dune unit were estimated relative to a fixed polygon that covers the entire system. Shoreline changes were mapped and analyzed using the tool DSAS (Digital Shoreline Analysis System) for ArcGIS (Thieler et al., 2009). The vegetated dune foot was used as indicator of shoreline position.

Flooding simulations have been used to delimit the flood-prone areas of the dune field, during normal and high water levels in the lagoon, coupled with sea level data. This information enables delineation of the more suitable areas for sand movement and/or vegetation growth.

Light detection and ranging (LiDAR) data were surveyed in 2010. LiDAR data were collected on ETRS89 datum and processed in ellipsoidal heights that were later transformed to orthometric heights (referred to the ADS) using the EGM08_REDNAP geoid model provided by the IGN. The result was projected into ED50, UTM zone 29N. A DTM (digital terrain model) was generated by linear interpolation of irregular points using the Delaunay triangulation, with a spatial resolution of 0.25 m.

Water elevation was monitored at 5-minute intervals with a Pressure Transducer (Seabird SBE 39 and AQUALogger 520 PT) during 2010 and 2011. The devices were deployed in the lagoon and in the open sea to register tidal and freshwater fluctuations. Additionally, direct measurements of water elevation were taken during high water level episodes in the dune field depressions. Water fluctuations have been simulated over the DTM using the observed and recorded water levels, to obtain the flood-prone areas in the sand barrier.

3.2. Ground Penetrating Radar (GPR)

Ground Penetrating Radar is a valuable non-invasive geophysical tool particularly suitable for the study of the internal structures in a variety of coastal settings (Bristow et al., 2000; Neal and Roberts, 2001; Jol et al., 2003; Costas et al., 2006; Derickson et al., 2008; Clemmensen et al., 2009; Buynevich et al., 2010; Girardi and Davis, 2010). A GPR system using a dual frequency antenna (600 and 200 MHz) from the IDS-GPR was used to image the subsurface. The 200 MHz results were chosen as the best compromise between penetration depth and event resolution for sedimentary materials (Jol et al., 2003). Geophysical data were synchronized to a RTK-GPS. 2D GPR surveys were designed to provide the record of blowout evolution by exploring the concave windward slope and crest of the blowout (Fig. 1). The 2D profile was collected with a distance interval between traces of 0.1 m and 0.25 samples/ns. The 2D data processing was carried out using REFLEXW by Sandmeier software following the sequence of steps proposed by Neal (2004), which includes zero time correction, signal-saturation correction, applications of gains and filter, velocity profile estimates, static corrections and migration. Radar-wave velocities were calculated using the interactive hyperbola-adaptation method. A velocity of 0.12 m/ns was estimated for the upper part of the profiles corresponding to dry sand, which matches the common values found in the literature (Reynolds, 1997; Costas et al., 2006; Girardi and Davis, 2010). A second typical velocity value of 0.06 m/ns was assumed for the saturated zone (SSI, 1993; Baker and Jol, 2007). Water table depths were ground-truthed with sediment cores collected using a TESS-1 suction corer (Méndez et al., 2003) and auger borings. Additional sediment cores were collected to ground-truth radar reflections. For that, the cores were described and sampled every 10 cm. All cores were corrected for compaction considering penetration depths. A non-homogenized fraction of approximately 1 g was used for grain-size analysis conducted using a Coulter LS100 laser granulometer.

Acquisition of 3D GPR data in aeolian environments provides a complete imaging of the internal geometry of the dune foresets and reveals structures that otherwise could be hidden (Bristow et al., 2007; Girardi and Davis, 2010). In this work, 3D GPR data were collected at the depositional lobe of the blowout with a dual frequency antenna (600 and 200 MHz), spaced 5 cm apart within a 10.5 m × 11 m grid (Fig. 1). The 3D data acquisition was performed following the typical approach for 3D seismic data consisting of an offset-circular pattern to ensure a complete coverage. These data were firstly processed within Sandermeier's REFLEXW software applying the same procedures as for the 2D data. Once processed, the data were exported to Landmark Pro software to build a 3D cube. Interpretation was undertaken with Kingdom SMT software.

3.3. Observed and simulated wind data

A wind series from A Coruña meteorological station, located 55 km to the northeast of the study area, was used to characterize the wind regime for the last seven decades (Fig. 1). The data spans a time interval between 1940 and 2011 (with a 6-hour interval record from 1940 to 1990 and hourly intervals from 1990 to 2011). The variability of three wind directions which impact on the study area was evaluated, i.e. SW, NW and NE. Overall trends were obtained from this long timeseries by smoothing the data using running averages to remove the seasonal cycle. Additionally, this dataset was used to identify the occurrence of storm events assuming that the passage of synoptic-scale storms is associated with SW strong winds (Lozano et al., 2004; Clarke and Rendell, 2009).

To establish the impact of the large-scale atmospheric modes prevailing at NA and controlling the western European climate on the local winds, we have used the surface wind field provided by a high-resolution (10 km) regional climate. This simulation spans a 49-year period between 1959 and 2007 with hourly resolution, and covers homogeneously the whole Iberian Peninsula and surrounding areas widely including the target region. This database allows evaluation of the spatial distribution of the wind regime in great detail and characterization of the wind series for the specific location of the studied dune field, which has been done at the monthly timescale after averaging from the hourly data. The simulation was obtained through dynamically downscaling reanalysis and analysis data using the Mesoscale Model MM5 (Grell et al., 1995). The ERA40 reanalysis (Uppala et al., 2005) was used to initialize and drive the MM5 model for the period in which it is available (i.e. 1959–2002); analysis data from the European Center for Medium Range Weather Forecast (ECMWF) were used afterward to complete the simulation up to 2007. The MM5 setup was chosen to accurately reproduce the local climatological features based on previous sensitivity tests (Jerez et al., 2010, 2012) which has been also employed in several MM5-based studies over the Iberian Peninsula (Gómez-Navarro et al., 2010, 2011). Vertically, a dense layer-structure with 27 inhomogeneous levels (more closely spaced near the surface) was considered up to 100 hPa. Each of the 49 years composing the whole simulated period was integrated in an individual continuous run given a spin-up period of one month to the model, which is good enough to prevent the influence of errors in the initialized variables (model initialization is performed with reanalysis data) and the noise in the early model outputs (Christensen, 1999; Giorgi and Bi, 2000). The suitability of this dataset for the purposes of this study has been highlighted elsewhere (Lorente-Plazas, 2010; Lorente-Plazas et al., 2011; Jerez et al., submitted for publication) and has been already used for different applications (Costas et al., 2012).

As a major novelty of this work, the role of three large-scale teleconnection modes of atmospheric circulation (NAO, EA and SCAND) has been explored, as they are the main drivers of the wind field in western Europe (Trigo et al., 2002; Martín et al., 2011), and the storminess index in the study area (Trigo et al., 2008).These teleconnections, which are independent, consist of dipolar patterns clearly visible in the Sea Level Pressure (SLP) in the NA, having simultaneously associated high and low pressure systems at different locations. The positive phase of the NAO is characterized by positive anomalies in SLP around the Azores Islands and negative anomalies in SLP near Iceland. The EA is structurally similar to the NAO but its anomaly centers are displaced southeastward to those characteristics of the NAO pattern. For this reason, the EA pattern is often interpreted as a “southward shifted” NAO pattern. However, the lower-latitude center contains a strong subtropical link in association with modulations in the subtropical ridge intensity and location. This subtropical link makes the EA pattern substantially distinct from its NAO counterpart. Finally, the SCAND has associated positive SLP anomalies over Scandinavia, with weaker centers of opposite sign over western Europe and eastern Russia/western Mongolia; see Fig. 6 in Trigo et al. (2008). The temporal evolution of these patterns can be characterized (at the monthly scale) by numerical indices retrieved here from the Climate Prediction Center from the National Oceanic and Atmospheric Administration (http://www.cpc.ncep.noaa.gov/data/teledoc/telecontents.shtml). Positive values of these indices correspond to intense dipoles in the associated SLP patterns and negative to softened dipoles. Here we consider positive mode phases those months characterized by index values above 0.5 and negative mode phases when the corresponding index value lies below −0.5.

4. Results

4.1. Morphological dune changes since the 1940s

The sequence of all aerial photographs available for the study area from 1945 to 2008 is shown in Fig. 2. The aerial photographs display a clear increase in the vegetation cover between 1957 and 2008. The first available flight (1945) shows a significantly evolved vegetation cover following a southwest lineation, representing approximately 34% of the total fixed area. A large percentage of the vegetation disappeared in 1957 representing only the 27% of the total area. Vegetation decline was accompanied by the retreat of the shoreline at around 0.7 m/yr. From 1957 to 2008 the vegetation gradually expanded covering approximately 77% of the total dune field surface. A new shoreline retreat between 1971 and 1985 with values around 0.2 m/yr was estimated. In the 1985 aerial photograph, it was possible to identify the flooding of the lower areas and the development of erosive scarps at the dune foot. Shoreline retreat during this time interval coincided with the passage of two hurricanes, downgraded to tropical cyclones by the time they reached Galicia, but still causing a large impact on the Galician coast. The tropical cyclone of 1978 caused two deaths and the destruction of several coastal infrastructures by strong waves accompanied by strong winds. Tropical cyclone Hortense hit land in 1984, resulting in numerous victims and the destruction of several constructions. This storm was responsible for winds higher than 200 km/h and torrential rainfall. The effect of these events provoked a sudden sea level over-elevation (storm surge) that could eventually explain the erosive scarps detected in the aerial photography of 1985. The same could explain the anomalous water table elevation, which caused the flooding of the lower zones. Since then, vegetation expansion accelerated (Fig. 2).

By 1985, well-developed erosive aeolian features (blowouts) were identified. Indeed, geomorphological aspects suggest that most of the aeolian forms active today were formed prior to 1985. To ensure a better understanding of the initiation and evolution of these aeolian forms a detailed analysis of a well-preserved blowout was completed. Fig. 3 shows the evolution of the blowout as well as the wind direction derived from the sedimentary erosive forms. The base of the depositional lobe position was used to infer rates of blowout migration. During the period between 1985 and 2008 the blowout migrated 18.5 m, at rates

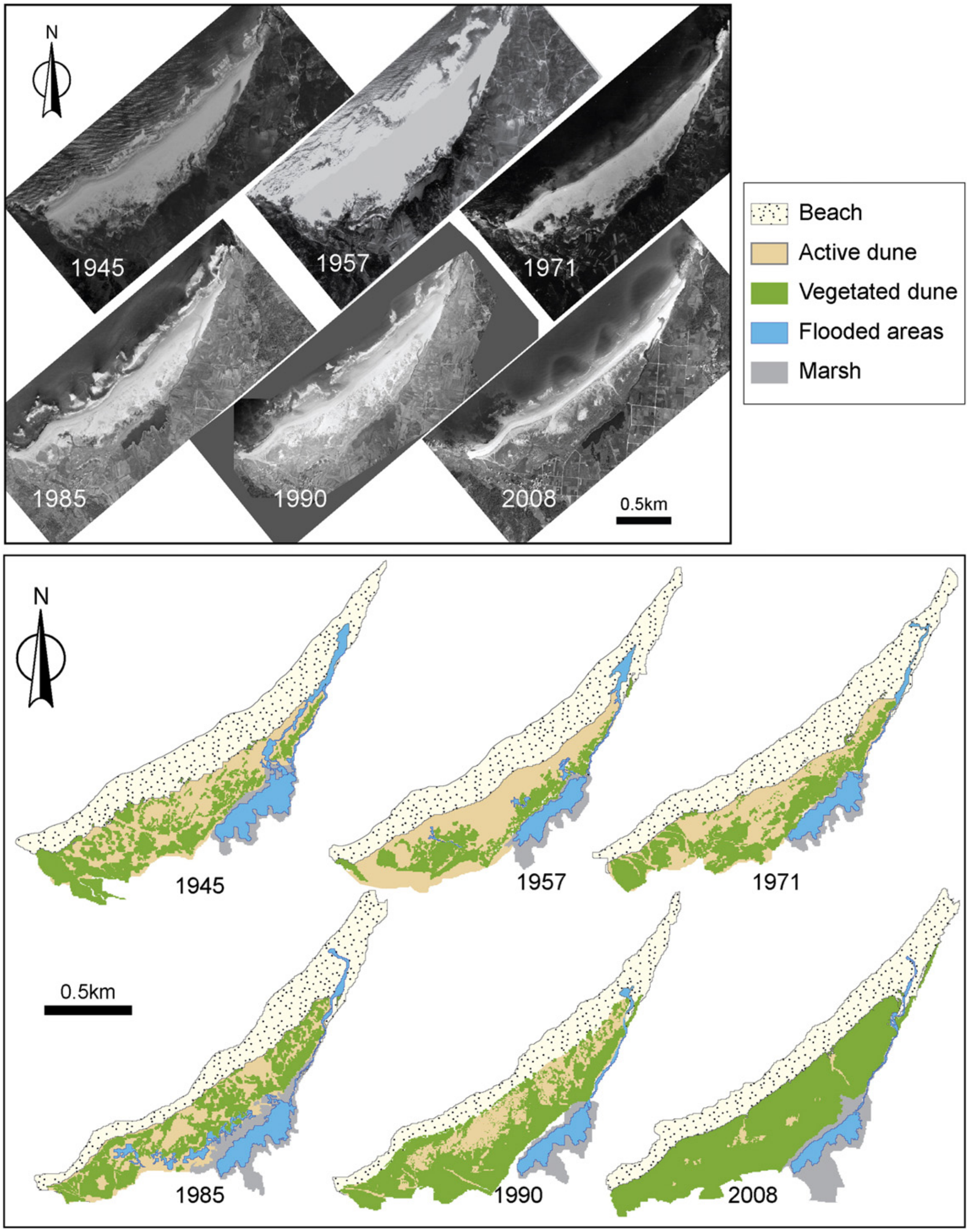

Fig. 2. Aerial photographs (upper panel) and distribution of the surface units identified (lower panel) from 1945 to 2008.

up to 0.8 m/yr. In 1985, the blowout presented an irregular shape with its long axis oriented NE to SW. Two deflation plains were recognized within the blowout showing different orientations, SE and S. Four years later, in 1989, the orientation of the blowout shifted to the south and the deflation plains became narrower and more localized. In 2003, the depositional lobes of the blowout were covered with vegetation, the blowout became smaller and two preferential branches were formed separated by a vegetated mound. More recently (i.e. in 2008), the blowout has become more active with a depositional lobe oriented to the SW, sharp erosional walls and well-developed rim dunes. The two branches, already detected in 2003, are clearly delineated at present.

Fig. 4 shows the flood simulations with variable tidal elevations and water levels in the lagoon. At present, the water level in the lagoon remains constant (2 m above ADS) during most of the year and the lower parts of the barrier are dry. However, if the water level in the lagoon reaches extreme values (around 3 m) due to peak inputs from rivers and rainfall, the lower parts of the barrier get flooded. This implies episodic inundation of the low areas during the year, reducing the surface susceptible of being blown. Therefore, sand movement appears restricted to the areas above 3 m over ADS. Vegetation expansion commenced after 1971 in the low-lying areas of the dune complex. These lower areas are prone to flooding when the water table rises to extreme values

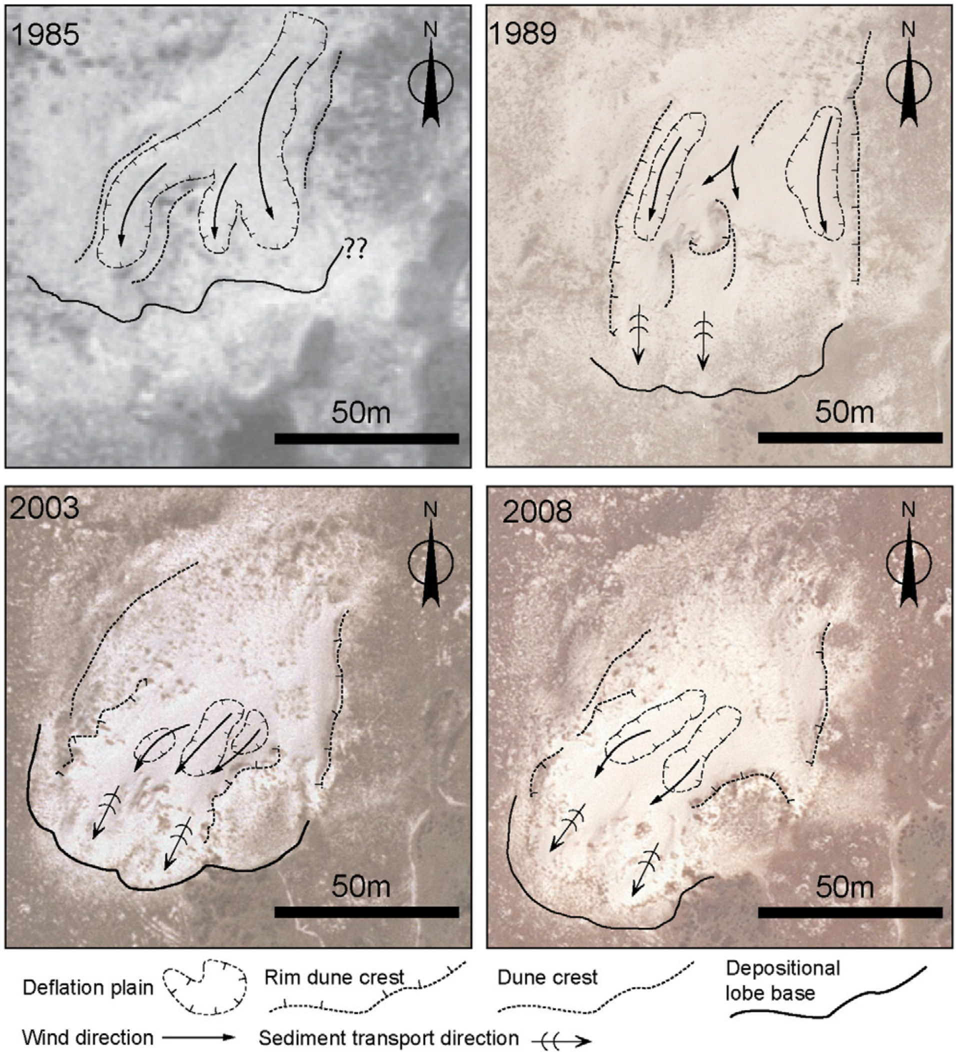

Fig. 3. Evolution of the active blowout between 1985 and 2008.

(Fig. 4), maintains high moisture contents when the water table falls, and favors vegetation expansion.

4.2. Blowout stratigraphy and evolution

Geophysical data focused on one of the active and best developed blowouts in the dune field. The 2D radargram is shown in Fig. 5. The transect runs from the windward slope to the crest and lee side of the feature (Fig. 1). GPR data were interpreted according to the principles of radar stratigraphy and following the terminology proposed by Neal (2004). Our results illustrate the depositional lobe of the blowout with reflections defining a set of cross-strata. A total of 9 units were identified within the depositional lobe, numbered sequentially from U1 to U9. Sediment cores collected within these units show that they consist of medium to coarse-grained, well-sorted quartz and carbonate sands. The presence of roots in the cores indicates the burial of

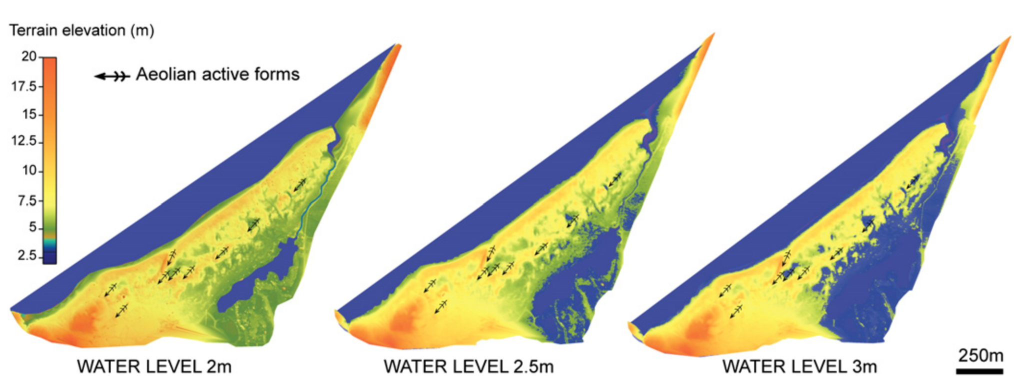

Fig. 4. Flood simulations in Traba coastal system. The results of the simulation shown from left to right the increase in the water table simulated from 2 m (common level in the lagoon) to 3 m (extreme water levels in the lagoon).

vegetation during the advance of the blowout. The occurrence of these vegetation remains was later associated with the diffractions observed in the GPR profile.

Different apparent dips were estimated within the different stratigraphic units (U2 to U9) as corresponding to pulses of blowout evolution. The apparent dips of units U2 to U9 ranged from 3° to 15°, respectively. This increase seems to be more accentuated from U4 upwards. Considering that the angle of repose of sand is generally about 30°, sedimentation very likely took place by grain flow processes rather than by grain fall. The net advance of the blowout is directed from NNE to SSW.

The depositional ages of the recent units can be obtained by crossing information from GPR and the latest aerial photographs. As the temporal resolution of aerial photography is not sufficient to cover all the changes observed in the GPR data, it was not possible to link the formation of units U1 to U3 with a specific aerial photograph, though they were apparently formed prior to 1985. However, we have been able to date major changes or pulses corresponding to the sedimentation of U4 to U9. U4 is interpreted to have been deposited between 1985 and 1989. U5 would be deposited between 1989 and 2003, U6 and U7 between 2003 and 2008, while U8 and U9 were formed between 2008 and 2011. All units became thinner and steeper with time. The changing dimensions and depositional timing of these units indicate that the pulses were not continuous in time.

U5 is the thickest unit and shows a complex internal configuration with two subunits. The lower subunit (SU5-1) was deposited at the lee slope being overlain by SU5-2. The internal configuration of this upper subunit resembles the rest of the identified units by contrast with the low internal definition of the lower subunit, dominated by discontinuous and convex reflectors with abundant diffractions and a poor internal coherence.

4.2.1. The 3D survey

The 3D grid was measured on top of the depositional lobe to decipher the last pulses of blowout evolution (Fig. 5). Six major bounding surfaces (S1 to S6) were identified above the water table (Fig. 6). The surfaces identified in the 3D cube were correlated with the boundaries of the units identified in the 2D line (Fig. 5). The 3D cube was used to estimate the migration directions of the units by picking the surfaces using the maximum curvature of the reflectors (Fig. 6).

The 3D cube illustrates the variability in the internal architecture of the depositional lobe and allows a better interpretation of the mechanisms involved in the deposition of the identified units. For this purpose, we have extracted several time slices from the cube cutting the depositional lobe at different depths (Fig. 6). The lower time slice was extracted at 3.6 m, and represents the base of the current depositional lobe. This time slice shows the preferential advance to the SSW marked by stronger amplitudes in the frontal part of the record. Elliptical forms with strong amplitudes were detected in this time slice that gradually disappeared upwards. These forms are surrounded by curved high-amplitude reflections interpreted with the support of aerial photographs and field observations as obstacles generated by vegetation mounds. These obstacles may interfere with sediment transport as they force the sand to settle around them promoting the formation of incipient sand bodies on the crest of the depositional lobe. The vegetation mounds are apparently inducing the vertical aggradation of the depositional lobe and the subsequent steeping of the leeward layers.

The next time slice, extracted at 4.8 m, images the complexity of SU5-1, already detected in the 2D GPR. In addition it provides some insights for the presence of discontinuous reflectors, which can be related to the presence of vegetation mounds as suggested by identified elliptical reflections. The SU5-2 is imaged in time slices at 5.2 m and 6 m. The configuration is more regular than in SU5-1, suggesting that the disturbing effect caused by the vegetation mounds diminishes upwards. Furthermore, the presence of the vegetation mounds induces the separation of the sand flow in two main branches with slightly different advancing directions to the S and WSW. In the last two time slices the reflectors representing U6 and U7 are more continuous, regular and closer, with higher dips.

4.3. The role of climatic variability

In addition to the general wind field pattern of the region, it is important to consider the role of the local orography, which may eventually determine or alter local wind directions. For the case of Traba dune field, the local orography enhances summer NE winds but shields the dune field from the impact of frequent winter SW

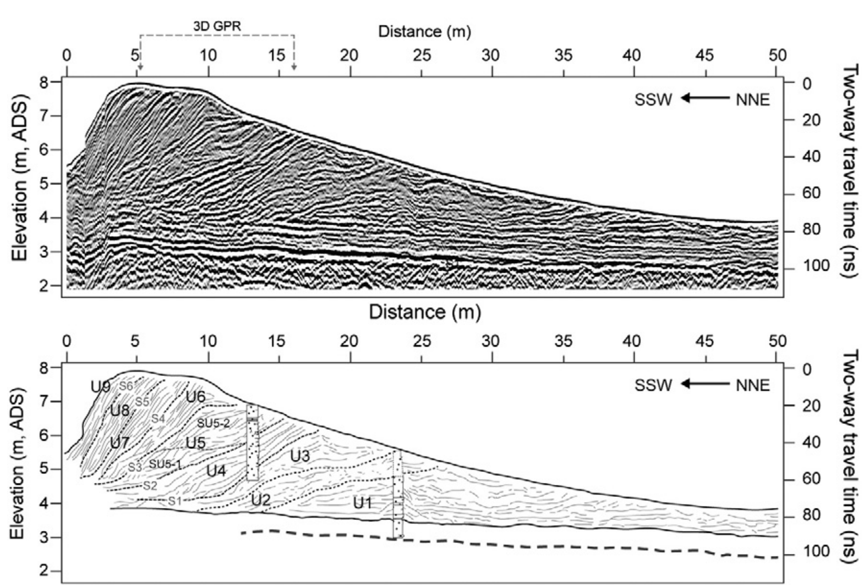

Fig. 5. 200 MHz GPR transect (upper panel) of the blowout and interpretation (lower panel). The black dashed lines represent the surfaces bounding the radar units and identified units within the depositional lobe of the blowout. The lower black dashed line represents the water table.

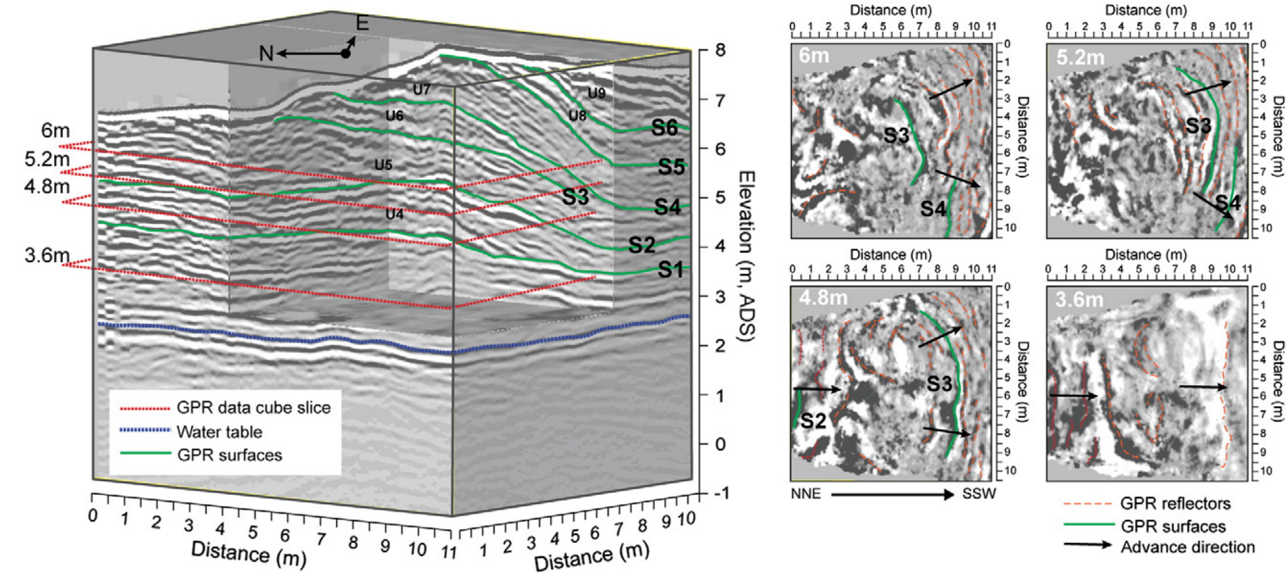

Fig. 6. Cube representation of the interior of the 3D survey at the depositional lobe of the blowout. Time slices at different depths are represented in the right panel.

winds. The three wind directions that are taken into account to analyze sand supply and transport in Traba are SW, NW and NE, as mentioned in Section 3.3. The evolution over time of these directions is shown in the upper panel of Fig. 7. The results show that dominant winds blow from NE and NW during summer and from SW during winter. The impact of these winds on the study area is summarized as follows: (1) SW winds are associated with the passage of winter storms, which bring high energy waves responsible for the offshore–onshore movement of sand in the beach, (2) NW winds during summer may transfer sediment from the beach to the adjacent dune, finally (3) NE summer winds can be related to the movement of sand within the dune field.

Two periods with distinctive wind regimes were identified. (1) The period between 1940 and 1960 was characterized by high values of wind speed and variability. The occurrence of winds above average during several consecutive years is indicative of a period with frequent and enhanced storminess (Fig. 7). (2) A second period after 1960 was characterized by lower peak values and variability. Wind speed gradually decreased up to 1970s, remaining with relatively low values ever since, in agreement with larger scale trends computed with other gridded

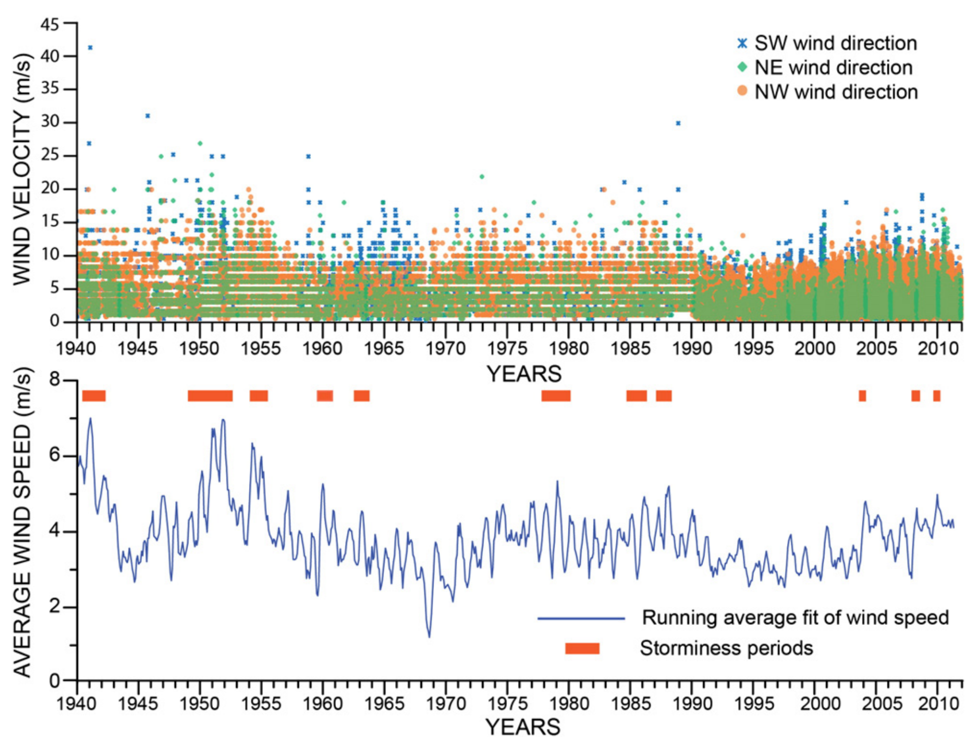

Fig. 7. Long-term wind record 1940–2011 (71 years) from A Coruña station: (upper panel) wind velocity (m/s) of SW, NW and NE directions recorded in the station; with a 6-hour interval record from 1940 to 1990 and hourly intervals from 1990 to 2011 (lower panel) monthly averaged wind speed (m/s), the orange bars show some examples of high storminess periods.

datasets (Trigo et al., 2008). Additionally, storm events were shorter than those of the previous period (Fig. 7).

To better explain the impact of the large-scale modes of atmospheric circulation on the local wind field, we have examined the wind for the specific location of Traba obtained from the high-resolution simulated wind field. In order to do this more effectively, a new system of coordinates was defined, resulting from a 45° rotation of the original coordinate system (with axes running east–west and south–north). The new axes are parallel and perpendicular to the directions of sand supply from the beach to the dune and sand transport within the dune. Thus, the component of the wind vector in the parallel-to-the-coast axis (named U10rot45, where 10 refers to the height in meters above the ground surface) represents winds blowing from the SW with positive values and NW with negative values. Similarly, the component of the wind vector in the perpendicular-to-the-coast axis (named V10rot45) represents winds blowing from the SE when it is positive and from the NW when it is negative.

The intra-annual variability of the temporal correlation between the large-scale circulation indices and both rotated wind components are shown in Fig. 8 (panels a and b). Additionally, we have constructed Linear Regression Models (LRM) for each rotated wind component considering the joint influence of NAO, EA and SCAND modes. The temporal correlation between these LRMs and both rotated wind components (also provided in Fig. 8a, b) highlights that NAO, EA and SCAND account for the 40–60% of the variability of the U10rot45 and the V10rot45 series in summer, rising to an 80% in winter in the case of U10rot45. According to this figure, the two most important circulation modes for the wind field are clearly identified as the EA and NAO patterns (with a predominance of the EA). Nevertheless, the influence of SCAND in the LRM is considered decisive to reach the high levels of explained variance mentioned above. The impact of these three modes in the mean values of the analyzed wind components was assessed by comparing the average values of U10rot45 and V10rot45 obtained from months characterized with positive or negative phase events of the various modes (Fig. 8c–h). As expected from the former analysis based on the A Coruña data set, U10rot45 and V10rot45 are predominantly positive in winter changing to negative values in the summer months. These results stress the key role played by the summer season when both sand supply to the dune and movement within the dune use to occur. This behavior is observed irrespective of the phase of the various modes. However, positive NAO, negative EA and negative SCAND enhance the intensity of the wind blowing from the NE in summer promoting the movement of the sand within the dune. On the contrary, negative NAO, positive EA and positive SCAND phases are bound to favor the NW winds and the sand supply from the beach.

Fig. 9 shows the impact of the various modes of atmospheric circulation on the summer season wind field (direction and module). The same figure highlights the opposite pattern displayed by EA and NAO modes and provides useful clues on the appropriate combination of modes to explain the wind field; positive NAO, negative EA and negative SCAND modes explain the occurrence of winds blowing from the NE, having the opposite combination of phases for NW winds.

Finally, Fig. 10 combines the results of the climate simulations for summer season (NAO, EA and SCAND index variability, and U10rot45 and V10rot45 series) and the observed morphological changes in the dune field. From this information, we could tentatively refine the deposition timing of the different radar units presented in Section 4.2. Favorable conditions for blowout advance (i.e. NE winds) occur during summers dominated by the negative phases of both EA and SCAND modes and positive NAO (Fig. 9). Following this rationale, we could assume that deposition of units U1 to U3 took place during the period between 1972 and 1980, which fulfill the criteria of enhanced NE winds. Even though the SCAND presents a positive phase during this period, it is not enough to cancel the effect of the other circulation modes. In addition, higher values of U10rot45 facilitate sand movement. The peak of U10rot45 between 1985 and 1987, coincident with a negative SCAND, could be responsible for the deposition of U4. Conversely, the deposition of U5 appears to occur under different combinations of summer circulation modes favoring the coexistence of vegetation growth and blowout advance, which in turn could explain the more complex internal structure of this unit.

5. Discussion and conclusions

5.1. Dune stabilization and reactivation

Shifts in key climate variables (wind and precipitation) can leave significant traces in dune fields as dune evolution is strongly linked to the behavior of the atmospheric system. However, the impact that atmospheric variability patterns have on the wind field regimes, directly affecting the dunes, has not been evaluated properly in many previous studies. Here, we have examined the impact of several relevant patterns of atmospheric circulation variability on the local wind field regime, which in turn forces the movement of sand in the dune. Therefore, we have not restricted our analysis to the NAO index, but have also accounted in this assessment the impact produced by major large-scale circulation modes affecting Iberia, i.e. the EA and SCAND patterns. Moreover, we have considered the role played by these three patterns during both winter and summer seasons, as both contribute through different complementary processes.

The recent evolution of the study area was marked by discernible changes in the vegetation cover. These changes have been related to different episodes of aeolian activity and dune stabilization. In the fifties the dune entered a phase of aeolian activity coincident with a decrease in vegetation cover (Fig. 2). Traditionally, an attempt has been done to link phases of dune reactivation and building to oscillations in the relative sea level (RSL), which in turn control sand supply. As RSL falls, the width of the emerged beach increases, enhancing the transference of sand from the beach to the dune (Clemmensen et al., 1996; Wilson et al., 2001; Bauer and Davidson-Arnott, 2002). Conversely, some authors have observed enhanced sand supply from beaches to dunes during RSL rise (Aagaard et al., 2007; Szkornik et al., 2008). Yet, in all these examples, the increase of sediment supply was ultimately related to the effect that storms may have on coastal currents or windiness regardless of RSL change (Clarke and Rendell, 2009).

In the NW of the Iberian Peninsula, a period of enhanced storminess was recorded during the 1950s associated to frequent SW winds (Fig. 7). This situation is coherent with the prevalence of persistent negative modes of the NAO index, which in turn is the principal contributor for the resultant wind regime during winter. Under these conditions, remobilization of large volumes of sand in the beach occurs due to the passage of energetic storms and waves. This sand may ultimately become available to favorable NW winds during summer. During summer, the wind field is explained by a more complex combination of atmospheric circulation modes, being the EA the major contributor. Interestingly, the favorable frequent NW winds that are ultimately responsible for the transference of sand from the beach to the dune, are compatible with the summer positive EA, negative NAO and positive SCAND, that are all quite similar (Fig. 9).

Following this period of enhanced storminess, a progressive expansion in vegetation cover was observed (Fig. 2) coincident with a gradually wind speed deceleration (Fig. 7). Since the earliest 1970s, vegetation growth concentrated in the low-lying areas, which became more stable matching the trends observed in other European systems (Bailey and Bristow, 2004; Costas et al., 2006; Arens et al., 2008; Jackson and Cooper, 2011). However, the observed shift in the wind field regime cannot explain by itself the progressive stabilization of the dune. Wind speeds, recorded since 1985, hold sufficient kinetic energy for sand entrainment (Figs. 7, 10). Indeed, if we assume that wind velocity at the height of 10 m in the study area is comparable to the raw data recorded in the meteorological station, we could assert

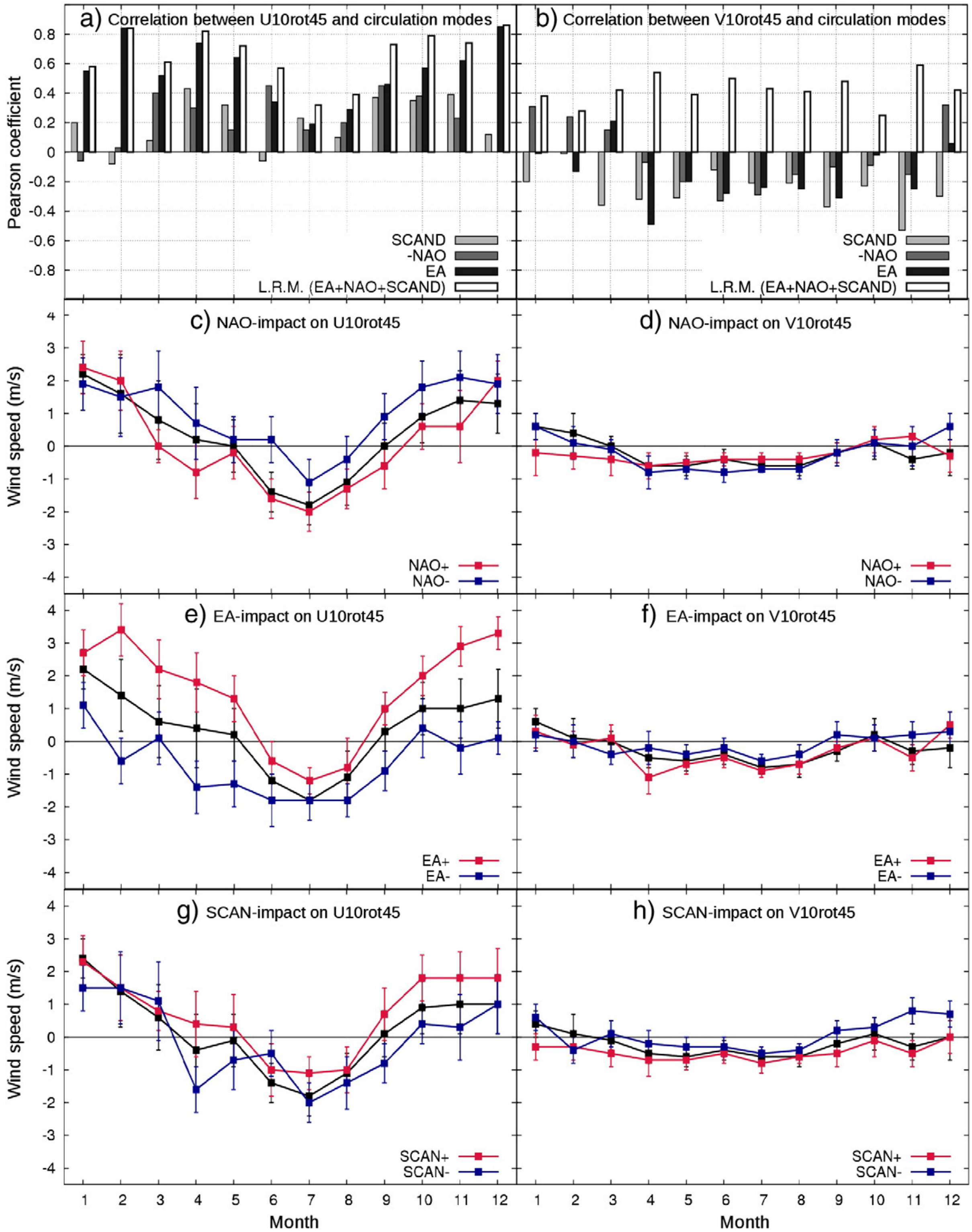

Fig. 8. Monthly timescale correlation of the role of NAO, EA and SCAND on the interannual variations of NE and NW components of the wind (U10rot45 and V10rot45 respectively) obtained with the simulated wind series for the specific location of the dune field. (a–b) Correlation between the NAO, EA and SCAND circulation modes with the wind components U10rot45 and V10rot45 (with negative values indicating that the wind blows from the NE and the NW in each case). Panels c and d show the impact of the three phases of NAO index in the mean values of the U10rot45 and V10rot45 wind components respectively. Panels e–f and g–h show the impact of the other two atmospheric circulation modes in the wind components (EA and SCAND respectively).

that shear velocities may exceed threshold values for sand entrainment. Estimated shear velocities based on the law of the wall (Von Kármán, 1930) may reach values higher than the theoretical threshold shear velocities for the entrainment of the local mean grain size (0.3–0.4 mm), in accordance with values suggested by Liu et al. (2006). Therefore, other factors must be considered to explain dune stabilization, namely sand availability.

Sand availability in aeolian dunes can be controlled by the elevation of the water table, which has been suggested as a major contributor for dune fixation (David et al., 1999; Gutiérrez-Elorza et al.,

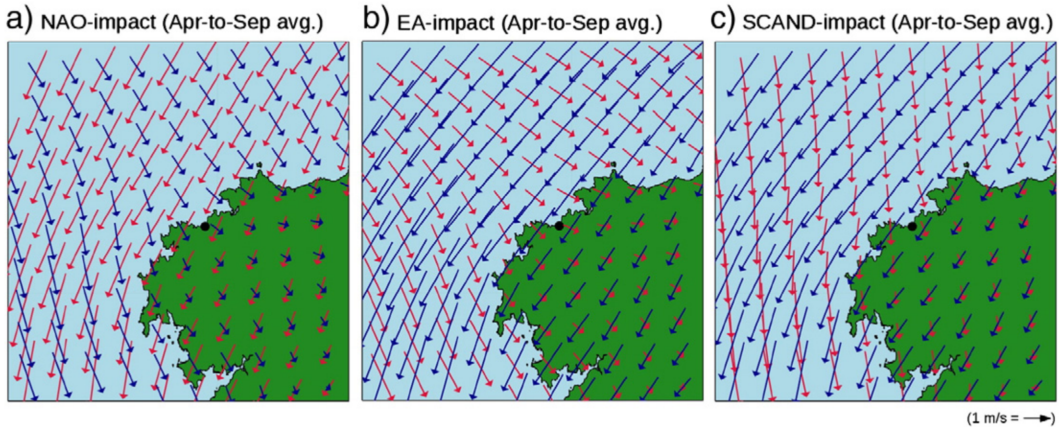

Fig. 9. Wind field patterns during the positive (red arrows) and negative (blue arrows) phases of EA, NAO and SCAND during the summer months (April to September).

2005). Water table oscillations change the moisture levels in the dune controlling sand entrainment, which can only occur above a threshold value of elevation above water table. In Traba, the dune field remained active before reaching the elevation threshold below which the dune was fixed. The areas that remain active are shaped by NE winds during summer season. Such winds are explained, to a large extent, by the occurrence of negative phases of both the EA and the SCAND and the positive phase of the NAO.

In summary, it is recognized that aeolian activity depends on sand supply from external sources and/or availability of sand in the system; it is then expected that if sediment supply is interrupted then the coastal dune tends to stabilize. In Traba, like in other areas of SW Europe, the climate variability inducing weaker and less frequent storms can be claimed as the more likely reason to explain the deficit of sediment input to the system and, in consequence, the expansion of the vegetation cover. Indeed, the episode of aeolian dune reactivation documented in Traba in the 1950s is the result of a series of processes triggered at the early stages by enhanced storminess.

Finally, it is worthy of mention that sediment availability can be controlled by the vegetation cover. In this regard, Tsoar (2005) presented a hysteresis curve which expresses that once the dune is stabilized, destabilization requires much more energy in terms of wind stress for vegetation destruction than what was needed for dune

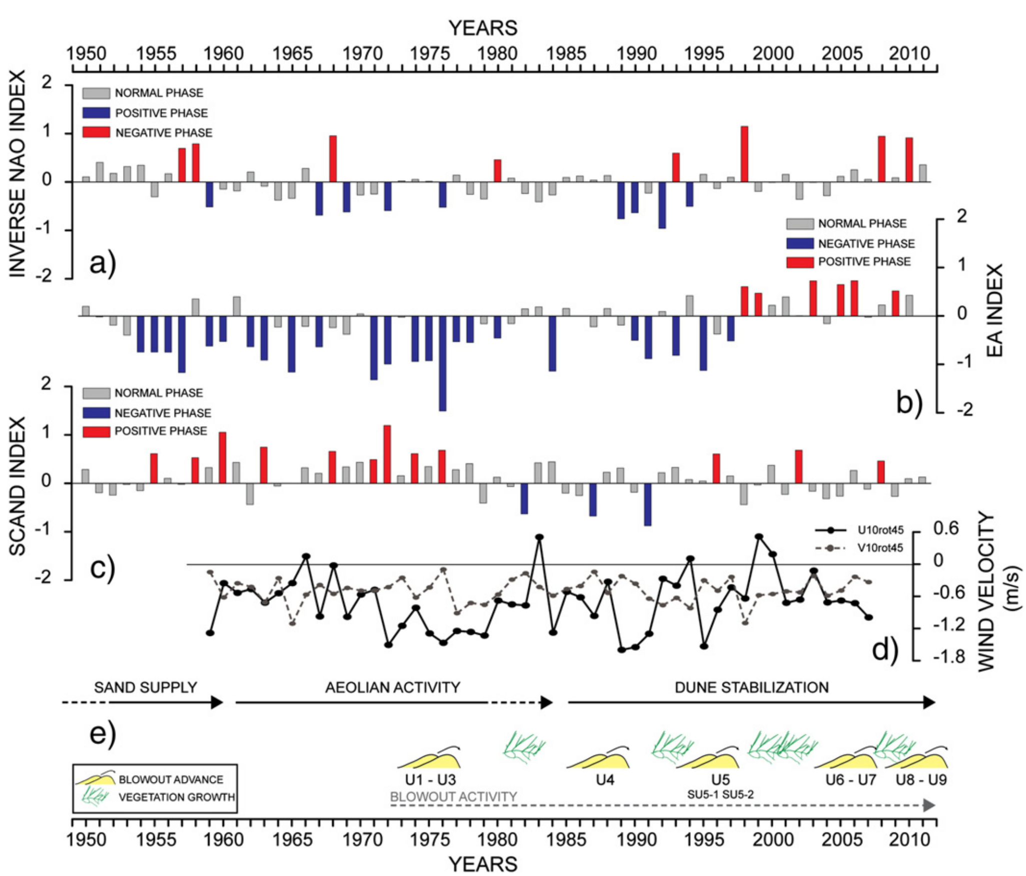

Fig. 10. Panels a to c show the mean summer values (April to September) of NAO, EA and SCAND. Panel d shows the mean wind velocity of two wind components. Panel e shows the blowout dune evolution and aeolian activity pulses.

fixation. This fact could help to explain the stabilization of Traba dune field under present quieter conditions of wind power once vegetation expanded.

In other areas of the European coast the relation between the NAO index and the coastal dynamics has been carefully explored. Chaverot et al. (2008) found that the impact of the NAO over the storm regime changed spatially along the French coast with regions where the impact of the NAO was negligible. In the coast of the United Kingdom, Pye and Blott (2008) suggested that major changes in coastal systems are due to the variability in the frequency and magnitude of storms, surges and extreme high tides. Shoreline retreat was documented by Costas and Alejo (2007) in NW Spain during the 1950s and related to a persistent negative mode of the NAO accompanied by severe storms and RSL rise. Enhanced storminess was probably a large-scale feature and not just a local trend. Indeed, this pattern apparently extended to northern latitudes, even reaching the United Kingdom (Alexander et al., 2005). However, the variability of all these indicators presented a modest relationship with the NAO index. Our results emphasize that the use of the NAO index solely is neither able to explain the evolution of the wind field nor the coastal dunes in the NW of the Iberian Peninsula. The correlation between the three modes of atmospheric circulation and different wind seasonal directions explains the small and large scale processes in the coastal system. It should be noted that EA and NAO (with predominance of EA) hold the largest correlations with both wind components; however the inclusion of SCAND in the simple regression model is decisive to obtain acceptable values of explained variance. Indeed, the combination of the three modes is sufficient to explain circa 80% of the SW winter winds and about 60% of the summer variability (Fig. 8). The effect of the climatic modes on dune activity in our study area has a marked seasonal behavior.

We have shown that to understand the morphological changes and evolution of these coastal systems it is essential to study the combined role played by the most important circulation patterns and their intrinsic variability. Furthermore, this approach provides invaluable data for the construction of future predictive models aiming to facilitate management and preservation.

5.2. Remnants of past aeolian activity: the blowouts

Despite the gradual stabilization of the dune field, active aeolian forms (blowouts) were observed in recent aerial photographs. The causes and time of blowout initiation in Traba are unclear due to the lack of clear-cut evidence. The first evidence of blowout development was observed in the aerial photograph of 1985. However, the results of climatic simulations suggest that the propitious circumstances for blowout formation occurred near 1972, with enhanced summer NE winds. In the case of Traba, the area occupied today by the blowout was characterized by wind-induced lineations between 1945 and 1971. This pre-blowout dune morphology may have facilitated the subsequent blowout development through wind acceleration. The interaction between the airflow and the inherited topography has been explored in different works that combine to highlight the role of topography on blowout development through airflow acceleration (Carter, 1988, 1990; Pluis, 1992; Gares and Nordstrom, 1995; Hesp and Hyde, 1996; Hugenholtz and Wolfe, 2009; Smyth et al., 2011, 2012).

A set of units was identified internally representing periods of reactivation and migration of the blowout. Commonly, blowouts are characterized by punctuated displacements driven by short-term climate oscillations before they become fixed (Flor, 1984; Pluis, 1992; Neal and Roberts, 2001; Hesp, 2002; Dech et al., 2005; Girardi and Davis, 2010; González-Villanueva et al., 2011). The early stages (units U1 to U3, Fig. 5) are characterized by low angle reflectors. The absence of vegetation allowed the migration of the blowout, indicating considerable sediment availability (Fig. 11a). Afterwards, units U4 and U5 represent transitional stages deposited before 2003. These units are characterized by a complex internal structure with diffractions caused by roots. 3D GPR data show reflections with opposite curvatures suggesting obstacles that could eventually force the

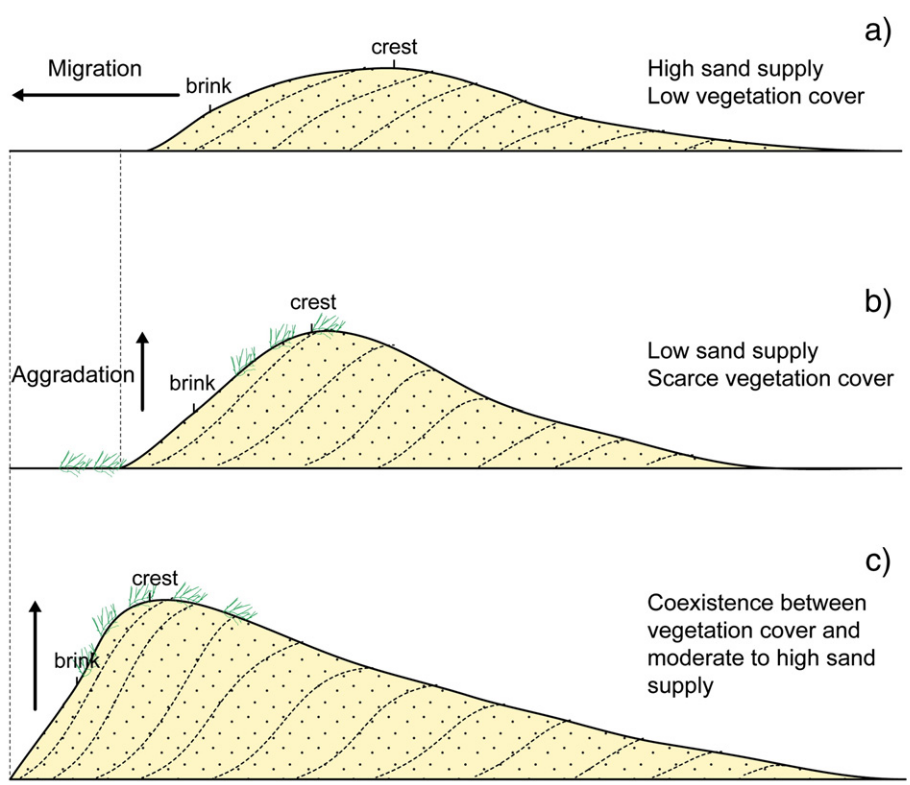

Fig. 11. Conceptual diagram illustrating the effect of sand supply and vegetation cover on blowout evolution.

sand to settle, as described in Girardi and Davis (2010). The sedimentation of these units agrees with the observed densification of vegetation between 1989 and 2003. This densification could be explained by the shift in wind regime recorded in A Coruña (Fig. 7) and the values of U10rot45 (Fig. 9), which show the shift from NE to SW winds during summer between 1996 and 2003. The obstacles interpreted as vegetation mounds and identified within the GPR data, may have promoted the vertical aggradation of these units, reducing the distance between the crest and the brink (Fig. 11b). The maturation of the blowout is represented by units U6 to U9 and coincides with an intensification of NE wind velocities recorded in A Coruña from 2003 to the present. The latter units are internally characterized by moderate to high angle cross-strata. The current surface of the depositional lobe is partially covered by vegetation, however the distance between the crest and the corresponding brink decreased over time (Fig. 11c). The morphological evolution of the depositional lobe differs from the results presented by Hugenholtz et al. (2008), who observed an increase in the distance between the crest and brink with the colonization of the dune.

To sum up, the resultant morphology, stratigraphy and advance direction of the blowouts are affected by environmental conditions like vegetation cover and wind magnitude and approach direction. Coexistence of vegetation and moderate to high sand supply provokes a change in the geometry of the lee slope, which becomes steeper. At the same time the distance between the crest and the brink reduces, and the internal stratigraphy shows moderate to high angle reflectors.

Acknowledgments

Thanks to Irene Alejo, Miguel Angel Nombela, Angel Mena, Carolina Gil, Raquel Sanchez, Tania Barragan, Corinne Perez and Paula Diz for their help with field work. Grants from 08MDS036000PR (Xunta de Galicia), PT2009-0067 (MICINN), 046/2007 (Ministerio de Medio Ambiente); SCARPS (PTDC/CTE-GIX/101466/2008) and CONTOURIBER (CTM2008-06399-C04-01/MAR, MICINN). Sonia Jerez and Ricardo Tirgo were supported by the project ENAC (PTDC/AAC-CLI/103567/2008) funded by the FCT in Portugal. Ricardo Trigo was partially supported by The Spanish Ministry of Science and Innovation trough project PALEONAO (CGL2010-15767). Thanks to Henrique Duarte and the Laboratório Nacional de Energía e Geología, to Landmark Graphics Corporation via the Landmark University Grant Program; Seismic Micro-Technology Inc. for Kingdom Suite software and the University of Vigo for grants. We would like also to acknowledge the MAR research group from of the University of Murcia for providing the data from the MM5 climate simulation and also to IGN, Spanish National Geographic Institute, for the LiDAR data.

Appendix A. Supplementary data

Supplementary data associated with this article can be found in the online version, at http://dx.doi.org/10.1016/j.geomorph.2012.12.019. These data include Google maps of the most important areas described in this article.

References

Aagaard, T., Davidson-Arnott, R., Greenwood, B., Nielsen, J., 2004. Sediment supply from shoreface to dunes: linking sediment transport measurements and long-term morphological evolution. Geomorphology 60, 205–224.

Aagaard, T., Orford, J., Murray, A.S., 2007. Environmental controls on coastal dune formation; Skallingen Spit, Denmark. Geomorphology 83, 29–47.

Alexander, L.V., Tett, S.F.B., Jonsson, T., 2005. Recent observed changes in severe storms over the United Kingdom and Iceland. Geophysical Research Letters 32, L13704.

Arens, S.M., Slings, Q.L., Geelen, L.H.W.T., Hagen, H.G.J.M.V.D., 2008. Implications of environmental change for dune mobility in the Netherlands, ICCD2007. International Conference on Management and Restoration of Coastal Dunes. Universidad de Cantabria, Santander, Spain.

Bailey, S.D., Bristow, C.S., 2004. Migration of parabolic dunes at Aberffraw, Anglesey, North Wales. Geomorphology 59, 165–174.

Baker, G.S., Jol, H.M., 2007. Stratigraphic Analyses using GPR GSA Books Science Editor, Special Paper 432. The Geological Society of America Inc., Colorado, USA.

Bao, R., Alonso, A., Delgado, C., Pages, J.L., 2007. Identification of the main driving mechanisms in the evolution of a small coastal wetland (Traba, Galicia, NW Spain) since its origin 5700 cal yr BP. Palaeogeography, Palaeoclimatology, Palaeoecology 247, 296–312.

Bauer, B.O., Davidson-Arnott, R.G.D., 2002. A general framework for modeling sediment supply to coastal dunes including wind angle, beach geometry, and fetch effects. Geomorphology 49, 89–108.

Bristow, C.S., Chroston, P.N., Bailey, S.D., 2000. The structure and development of foredunes on a locally prograding coast: insights from ground-penetrating radar surveys, Norfolk, UK. Sedimentology 47, 923–944.

Bristow, C.S., Duller, G.A.T., Lancaster, N., 2007. Age and dynamics of linear dunes in the Namib Desert. Geology 35, 555–558.

Buynevich, I., Bitinas, A., Pupienis, D., 2007. Reactivation of Coastal Dunes documented by subsurface imaging of the Great Dune Ridge, Lithuania. Journal of Coastal Research SI50, 226–230.

Buynevich, I.V., Filho, P.W.M.S., Asp, N.E., 2010. Dune advance into a coastal forest, equatorial Brazil: a subsurface perspective. Aeolian Research 2, 27–32.

Carter, R.W.G., 1988. Coastal Environments—An Introduction to the Physical, Ecological and Cultural Systems of Coastlines. Academic Press, London.

Carter, R.W.G.a.W.P., 1990. The geomorphological, ecological and pedological development of coastal foredunes at Magilligan Point, Northern Ireland. In: Nordstrom, Psuty, Norbert, Carter, Bill (Ed.), Coastal Dunes: Form and Process. Wiley, Chichester, pp. 129–157.

Chaverot, S., Héquette, A., Cohen, O., 2008. Changes in storminess and shoreline evolution along the northern coast of France during the second half of the 20th century. Zeitschrift für Geomorphologie, Supplementary Issues 52, 1–20.

Christensen, O.B., 1999. Relaxation of Soil Variables in a Regional Climate Model, 51.

Clarke, M.L., Rendell, H.M., 2009. The impact of North Atlantic storminess on western European coasts: a review. Quaternary International 195, 31–41.

Clarke, M., Rendell, H., Tastet, J.-P., Clave, B., Masse, L., 2002. Late-Holocene sand invasion and North Atlantic storminess along the Aquitaine Coast, southwest France. The Holocene 12, 231–238.

Clemmensen, L.B., Andreasen, F., Nielsen, S.T., Sten, E., 1996. The late Holocene coastal dunefield at Vejers, Denmark: characteristics, sand budget and depositional dynamics. Geomorphology 17, 79–98.

Clemmensen, L.B., Murray, A., Heinemeier, J., de Jong, R., 2009. The evolution of Holocene coastal dunefields, Jutland, Denmark: a record of climate change over the past 5000 years. Geomorphology 105, 303–313.

Costas, S., Alejo, I., 2007. Local and global influences on the evolution of a transgressive sand barrier: Cíes Barrier, Northwest Spain. Journal of Coastal Research SI50, 1121–1125.

Costas, S., Alejo, I., Rial, F., Lorenzo, H., Nombela, M.A., 2006. Cyclical evolution of a modern transgressive sand barrier in NW-Spain elucidated by GPR and aerial photo. Journal of Sedimentary Research 76, 1077–1092.

Costas, S., Jerez, S., Trigo, R.M., Goble, R., Rebêlo, L., 2012. Sand invasion along the Portuguese coast forced by westerly shifts during cold climate events. Quaternary Science Reviews 42, 15–28.

David, P.P., Wolfe, S.A., Huntley, D.J., Lemmen, D.S., 1999. Activity cycle of parabolic dunes based on morphology and chronology from Seward sand hills, Saskatchewan. Bulletin of the Geological Survey of Canada 223–238.

Davidson-Arnott, R.G.D., Law, M.N., 1996. Measurement and prediction of long-term sediment supply to coastal foredunes. Journal of Coastal Research 12.

Dech, J.P., Maun, M.A., Pazner, M.I., 2005. Blowout dynamics on Lake Huron sand dunes: analysis of digital multispectral data from colour air photos. Catena 60, 165–180.

Derickson, D., Kocurek, G., Ewing, R.C., Bristow, C., 2008. Origin of a complex and spatially diverse dune-field pattern, Algodones, southeastern California. Geomorphology 99, 186–204.

Devoy, R.J.N., Delaney, C., Carter, R.W.G., Jennings, S.C., 1996. Coastal stratigraphies as indicators of environmental changes upon European Atlantic Coasts in the late Holocene. Journal of Coastal Research 12, 564–588.

Flor, G., 1984. Estudio sedimentológico y morfológico de la duna costera "blowout" (Cabo Frouxeira, La Coruña). Trabajos de Geología, 14.

Gares, P.A., Nordstrom, K.F., 1995. A cyclic model of foredune blowout evolution for a leeward coast: Island Beach, New Jersey. Annals of the Association of American Geographers 85, 1–20.

Gaylord, D.R., Stetler, L.D., 1994. Aeolian-climatic thresholds and sand dunes at the Hanford site, south-central Washington, U.S.A. Journal of Arid Environments 28, 95–116.

Gimeno, L., Trigo, R.M., Gómez-Gesteira, M., 2011. Regional climate change in the NW Iberian Peninsula. Climate Research 48, 105–108.

Giorgi, F., Bi, X., 2000. A study of internal variability of a regional climate model. Journal of Geophysical Research 105, 29503–29521.

Girardi, J.D., Davis, D.M., 2010. Parabolic dune reactivation and migration at Napeague, NY, USA: insights from aerial and GPR imagery. Geomorphology 114, 530–541.

Gómez-Gesteira, M., Gimeno, L., deCastro, M., Lorenzo, M.N., Alvarez, I., Nieto, R., Taboada, J.J., Crespo, A.J.C., Ramos, A.M., Iglesias, I., Gómez-Gesteira, J.L., Santo, J.F., Barriopedro, D., Trigo, I.F., 2011. The state of climate in NW Iberia. Climate Research 48, 109–144.

Gómez-Navarro, J.J., Montávez, J.P., Jimenez-Guerrero, P., Jerez, S., García-Valero, J.A., González-Rouco, J.F., 2010. Warming patterns in regional climate change projections over the Iberian Peninsula. Meteorologische Zeitschrift 19, 275–285.

Gómez-Navarro, J.J., Montávez, J.P., Jerez, S., Jiménez-Guerrero, P., Lorente-Plazas, R., González-Rouco, J.F., Zorita, E., 2011. A regional climate simulation over the Iberian Peninsula for the last millennium. Climate of the Past 7, 451–472.

González-Villanueva, R., Costas, S., Duarte, H., Pérez-Arlucea, M., Alejo, I., 2011. Blowout evolution in a coastal dune: using GPR, aerial imagery and core records. Journal of Coastal Research SI64, 278–282.
Goodess, C.M., Jones, P.D., 2002. Links between circulation and changes in the characteristics of Iberian rainfall. International Journal of Climatology 22, 1593–1615.
Grell, G.A., Dudhia, J., Stauffer, D.R., 1995. A description of the fifth-generation Penn State/NCAR Mesoscale Model (MM5). NCAR Tech. Note TN398 STR, p. 138.
Gutiérrez-Elorza, M., Desir, G., Gutiérrez-Santolalla, F., Marín, C., 2005. Origin and evolution of playas and blowouts in the semiarid zone of Tierra de Pinares (Duero Basin, Spain). Geomorphology 72, 177–192.
Hesp, P., 2002. Foredunes and blowouts: initiation, geomorphology and dynamics. Geomorphology 48, 245–268.
Hesp, P.A., Hyde, R., 1996. Flow dynamics and geomorphology of a trough blowout. Sedimentology 43, 505–525.
Hugenholtz, C.H., Wolfe, S.A., 2009. Form–flow interactions of an aeolian saucer blowout. Earth Surface Processes and Landforms 34, 919–928.
Hugenholtz, C.H., Wolfe, S.A., Moorman, B.J., 2008. Effects of sand supply on the morphodynamics and stratigraphy of active parabolic dunes, Bigstick Sand Hills, southwestern Saskatchewan Geological Survey of Canada Contribution 20060654. Canadian Journal of Earth Sciences 45, 321–335.
Jackson, D.W.T., Cooper, J.A.G., 2011. Coastal dune fields in Ireland: rapid regional response to climatic change. Journal of Coastal Research SI64, 293–297.
Jerez, S., Montavez, J.P., Gomez-Navarro, J.J., Jimenez-Guerrero, P., Jimenez, J., Gonzalez-Rouco, J.F., 2010. Temperature sensitivity to the land-surface model in MM5 climate simulations over the Iberian Peninsula. Meteorologische Zeitschrift 19, 363–374.
Jerez, S., Montavez, J., Jimenez-Guerrero, P., Gomez-Navarro, J., Lorente-Plazas, R., Zorita, E., 2012. A multi-physics ensemble of present-day climate regional simulations over the Iberian Peninsula. Climate Dynamics 1–24.
Jerez, S., Trigo, R., Vicente-Serrano, S., Pozo-Vázquez, D., Lorente-Plazas, R., Lorenzo-Lacruz, J., Santos-Alamillos, F., Montávez, J., submitted for publication. The impact of the North Atlantic Oscillation on the renewable energy resources in southwestern Europe. Journal of Applied Meteorology and Climatology.
Jol, H.M., Lawton, D.C., Smith, D.G., 2003. Ground penetrating radar: 2-D and 3-D subsurface imaging of a coastal barrier spit, Long Beach, WA, USA. Geomorphology 53, 165–181.
Klijn, J., 1990. Dune forming factors in geological context. In: Bakker, T., Jungerius, P., Klijn, J. (Eds.), Dunes of the European Coasts: Geomorphology, Hydrology, Soils, pp. 1–13.
Lebreiro, S.M., Francés, G., Abrantes, F.F.G., Diz, P., Bartels-Jónsdóttir, H.B., Stroynowski, Z.N., Gil, I.M., Pena, L.D., Rodrigues, T., Jones, P.D., Nombela, M.A., Alejo, I., Briffa, K.R., Harris, I., Grimalt, J.O., 2006. Climate change and coastal hydrographic response along the Atlantic Iberian margin (Tagus Prodelta and Muros Ría) during the last two millennia. The Holocene 16, 1003–1015.
Liu, X., Dong, Z., Wang, X., 2006. Wind tunnel modeling and measurements of the flux of wind-blown sand. Journal of Arid Environments 66, 657–672.
Lorente-Plazas, R., 2010. Elaboración de una base de datos pseudoreal para la evaluación del potencial eólico para Minieólica. MSc Thesis, Universidad de Granada, Spain.
Lorente-Plazas, R., Montávez, J.P., Jerez, S., Gómez-Navarro, J.J., Garcia-Valero, J.A., Jiménez-Guerrero, P., Jiménez, P.A., González-Rouco, J.F., 2011. Regional characterization of the observed and modelled wind over Spain. 11th European Meteorological Society Annual Meeting and 10th European Conference on Applications of Meteorology (ECAM), Berlin.
Lozano, I., Devoy, R.J.N., May, W., Andersen, U., 2004. Storminess and vulnerability along the Atlantic coastlines of Europe: analysis of storm records and of a greenhouse gases induced climate scenario. Marine Geology 210, 205–225.
Martín, M.L., Valero, F., Morata, A., Luna, M.Y., Pascual, A., Santos-Muñoz, D., 2011. Springtime coupled modes of regional wind in the Iberian Peninsula and large-scale variability patterns. International Journal of Climatology 31, 880–895.
Martínez Cortizas, A., Pérez Alberti, A., 1999. Atlas Climático de Galicia. Conselleria de Medio Ambiente, Xunta de Galicia, Santiago de Compostela.
Méndez, G., Pérez-Arlucea, M., Stouthammer, E., Berensden, H., 2003. The TESS-1 suction corer: a new device to extract wet, uncompacted sediments. Journal of Sedimentary Research 73, 1078–1081.
Neal, A., 2004. Ground-penetrating radar and its use in sedimentology: principles, problems and progress. Earth-Science Reviews 66, 261–330.
Neal, A., Roberts, C.L., 2001. Internal structure of a trough blowout, determined from migrated ground-penetrating radar profiles. Sedimentology 48, 791–810.
Osborn, T.J., Briffa, K.R., Tett, S.F.B., Jones, P.D., Trigo, R.M., 1999. Evaluation of the North Atlantic Oscillation as simulated by a coupled climate model. Climate Dynamics 15, 685–702.
Pluis, J.L.A., 1992. Relationships between deflation and near surface wind velocity in a coastal dune blowout. Earth Surface Processes and Landforms 17, 663–673.
Provoost, S., Jones, M., Edmondson, S., 2011. Changes in landscape and vegetation of coastal dunes in northwest Europe: a review. Journal of Coastal Conservation 15, 207–226.
Pye, K., 1993. Introduction: the nature and significance of aeolian sedimentary systems. Geological Society, London, Special Publications 72, 1–4.
Pye, K., Blott, S.J., 2008. Decadal-scale variation in dune erosion and accretion rates: an investigation of the significance of changing storm tide frequency and magnitude on the Sefton coast, UK. Geomorphology 102, 652–666.
Quadrelli, R., Pavan, V., Molteni, F., 2001. Wintertime variability of Mediterranean precipitation and its links with large-scale circulation anomalies. Climate Dynamics 17, 457–466.
Reynolds, J.M., 1997. An Introduction to Applied and Environmental Geophysics. John Wiley, New York, USA.
Rodriguez-Fonseca, B., de Castro, M., 2002. On the connection between winter anomalous precipitation in the Iberian Peninsula and North West Africa and the summer subtropical Atlantic sea surface temperature. Geophysical Research Letters 29, 1863.
Sáenz, J., Zubillaga, J., Rodríguez-Puebla, C., 2001. Interannual variability of winter precipitation in northern Iberian Peninsula. International Journal of Climatology 21, 1503–1513.
Smyth, T.A.G., Jackson, D.W.T., Cooper, J.A.G., 2011. Computational fluid dynamic modeling of three-dimensional airflow over dune blowouts. Journal of Coastal Research S157, 314–318.
Smyth, T.A.G., Jackson, D.W.T., Cooper, J.A.G., 2012. High resolution measured and modelled three-dimensional airflow over a coastal bowl blowout. Geomorphology 177–178, 62–73.
SSI, 1993. Ekko-Tools User's Guide, Version 1.1, Technical Manual, 22. Sensors and Software, Inc., Mississauga, Canada.
Szkornik, K., Gehrels, W.R., Murray, A.S., 2008. Aeolian sand movement and relative sea-level rise in Ho Bugt, western Denmark, during the 'Little Ice Age'. The Holocene 18, 951–965.
Thieler, E.R., Himmelstoss, E.A., Zichichi, J.L., Ergul, A., 2009. Digital Shoreline Analysis System (DSAS) version 4.0—an ArcGIS extension for calculating shoreline change. U.S. Geological Survey Open-File Report.
Trigo, R.M., Osborn, T.J., Corte-Real, J.M., 2002. The North Atlantic Oscillation influence on Europe: climate impacts and associated physical mechanisms. Climate Research 20, 9–17.
Trigo, R.M., Pozo-Vázquez, D., Osborn, T.J., Castro-Díez, Y., Gámiz-Fortis, S., Esteban-Parra, M.J., 2004. North Atlantic oscillation influence on precipitation, river flow and water resources in the Iberian Peninsula. International Journal of Climatology 24, 925–944.
Trigo, R.M., Valente, M.A., Trigo, I.F., Miranda, P.M.A., Ramos, A.M., Paredes, D., García-Herrera, R., 2008. The impact of North Atlantic wind and cyclone trends on European precipitation and significant wave height in the Atlantic. Annals of the New York Academy of Sciences 1146, 212–234.
Tsoar, H., 2005. Sand dunes mobility and stability in relation to climate. Physica A: Statistical Mechanics and its Applications 357, 50–56.
Tsoar, H., Levin, N., Porat, N., Maia, L.P., Herrmann, H.J., Tatumi, S.H., Claudino-Sales, V., 2009. The effect of climate change on the mobility and stability of coastal sand dunes in Ceará State (NE Brazil). Quaternary Research 71, 217–226.
Uppala, S.M., KÅllberg, P.W., Simmons, A.J., Andrae, U., Bechtold, V.D.C., Fiorino, M., Gibson, J.K., Haseler, J., Hernandez, A., Kelly, G.A., Li, X., Onogi, K., Saarinen, S., Sokka, N., Allan, R.P., Andersson, E., Arpe, K., Balmaseda, M.A., Beljaars, A.C.M., Berg, L.V.D., Bidlot, J., Bormann, N., Caires, S., Chevallier, F., Dethof, A., Dragosavac, M., Fisher, M., Fuentes, M., Hagemann, S., Hólm, E., Hoskins, B.J., Isaksen, L., Janssen, P.A.E.M., Jenne, R., McNally, A.P., Mahfouf, J.F., Morcrette, J.J., Rayner, N.A., Saunders, R.W., Simon, P., Sterl, A., Trenberth, K.E., Untch, A., Vasiljevic, D., Viterbo, P., Woollen, J., 2005. The ERA-40 re-analysis. Quarterly Journal of the Royal Meteorological Society 131, 2961–3012.
Vilas, F., Rolán, E., 1985. Caracterización de las lagunas costeras de Galicia, N.W. Peninsula Ibérica. España., Actas I° Congreso Ibérico de Quaternario. Universidade de Lisboa, Lisboa, pp. 253–268.
Von Kármán, T., 1930. Mechanische Ähnlichkeit und Turbulenz. Nachrichten von der Gesellschaft der Wissenschaften zu Göttingen, Fachgruppe 1 (Mathematik), 5, pp. 58–76.
Wilson, P., Braley, S.M., 1997. Development and age structure of Holocene coastal sand dunes at Horn Head, near Dunfanaghy, Co Donegal, Ireland. The Holocene 7, 187–197.
Wilson, P., Orford, J.D., Knight, J., Braley, S.M., Wintle, A.G., 2001. Late-Holocene (post-4000 years BP) coastal dune development in Northumberland, northeast England. The Holocene 11, 215–229.